Low-lying states of transverse substituted *trans*-polyacetylene and *trans*-polyacetylene: A comparative DMRG study

Manoranjan Kumar[1,2] and S. Ramasesha[1]
[1]*Solid State and Structural Chemistry Unit, Indian Institute of Science, Bangalore 560012, India*
[2]*Department of Chemistry, Princeton University, Princeton, New Jersey 08544, USA*
(Received 25 October 2009; revised manuscript received 24 December 2009; published 25 January 2010)

The density-matrix renormalization group (DMRG) method is used for a comparative study of low-lying excitations in *trans*-polyacetylene (t-PA) and transversely substituted t-PA (TS-t-PA). We have employed the Pariser-Parr-Pople model Hamiltonian which incorporates long-range electronic correlations to model these systems. We find some fundamental differences in the excited states of the t-PA and TS-t-PA. We find that the lowest two-photon allowed excited state in TS-t-PA is not made up of two triplet excitons and the gap to this state is nonzero even for undimerized chains in the thermodynamic limit. Contrary to earlier results for the Hubbard model, we find that the lowest two-photon state is always below the first optically allowed state in all the systems studied here making TS-t-PA systems only weakly fluorescent materials. Nonresonant tumbling averaged linear and third harmonic generation optic coefficients of TS-t-PA systems are also much smaller than that of t-PA.

DOI: 10.1103/PhysRevB.81.035115 PACS number(s): 71.10.Fd, 71.45.Gm, 31.15.ap

I. INTRODUCTION

The quest for strongly photoluminescent (PL) conjugated material has been a frontier area of research in the last few decades. In particular, there are efforts to design a light emitting conjugated system with an optical gap less than 1 eV for optical telecommunication purposes.[1–4] To achieve this, the conjugated system should have the lowest optically allowed excited state lying about 1 eV above the ground state (gs) with no other excited singlet state below this state. If an optically forbidden state exists below the optically allowed state, the system would not be fluorescent, because the molecule in the optically allowed excited state would internally convert rapidly (in a few hundred femtoseconds) to the lowest excited state which is optically forbidden, according to the Kasha rule[5] and from the forbidden state the molecule would fluoresce only weakly. Thus, the PL efficiency of a conjugated system would be determined by the ordering of the energy levels of the optically allowed and optically forbidden singlet excited states. If a polymer has an inversion center, the gs usually lies in the A_g space and $E(2A_g)$ is the gap to the first excited state in A_g space. $E(1B_u)$ is the energy gap to the first dipole allowed excited state. The condition for strong PL is $E(2A_g) > E(1B_u)$ by the Kasha rule since by symmetry, the transition dipole vanishes between states in the same space and hence radiative emission is forbidden from the $2A_g$ state.[5,6] Weak PL of *trans*-polyacetylene (t-PA) is an excellent example of this mechanism. Many conjugated polymers have been synthesized in which $E(2A_g) > E(1B_u)$ and consequently they show strong PL. This class of polymers has been synthesized by either replacing hydrogen of t-PA chain by phenyl groups or by introducing phenyl rings in the conjugated backbone as in polyphenylacetylene (PPA) and polyparaphenylenevinylenes (PPV).[7,8]

To physically understand the relative energies of $2A_g$ and $1B_u$ states, conjugation topology, strength of electron correlations, and the number of conjugated units in the molecule all need to be taken into account.[9] For example, although PPV is a conjugated system with p^z orbitals of sp^2 carbon in conjugation, similar to t-PA, PPV is strongly fluorescent while t-PA is not. This has been traced to the large effective dimerization in PPV, because parasubstituted phenyl rings in conjugation can be replaced by strongly dimerized butadiene with extended delocalization and localized ethylene π system. It has been shown both from exact diagonalization studies and density-matrix renormalization group (DMRG) studies that the $2A_g$ state in t-PA moves above $1B_u$ state as the dimerization δ in the t-PA chain increases, even if the correlation strengths remain unaltered.[6,10–12] In substituted t-PA, crossover of the $2A_g$ and $1B_u$ states can also be achieved by tuning the strength of electron correlations, with all the other parameters held fixed. Since in t-PA, the $2A_g$ excitation is a localized excitation while $1B_u$ excitation is an extended excitation, it has also been shown that, for intermediate correlation strengths, the $1B_u$ state descends below the $2A_g$ state as the length of the π conjugation is increased.

Shukla and Mazumdar[13] postulated that t-PA with the H atoms substituted by long conjugated side chains would have a low optical gap perhaps in the range of 1 eV. They reasoned that the $1B_u$ exciton in the transversely substituted t-PA (TS-t-PA) would delocalize along the side chain leading to its stabilization and concomitant lowering of the optical gap. Shukla and Mazumdar[13] modeled the optical properties of poly diphenyl polyacetylene (PDPA) using the Pariser-Parr-Pople (PPP) model within a restricted configuration interaction calculation involving only singly excited Slater determinants. Their study showed that the $2A_g$ state lies above the $1B_u$ state. To understand the effect of electron correlation on substituted t-PA, they took a modified structure, namely, poly(diethylacetylene) (PDEA) and used exciton basis to calculate the properties.[14] Recently, Yan and Mazumdar have used DMRG methods for modeling the PDEA system using a Hubbard model.[15] They showed that $2A_g/1B_u$ crossover in the PDEA takes place at a higher value of U/t compared to that of t-PA.

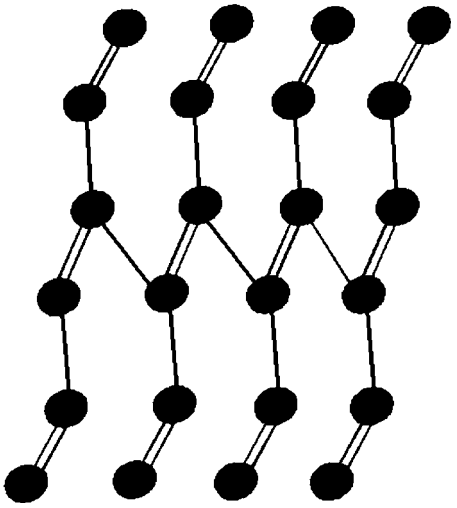

FIG. 1. Chemical structure of an oligomer of PDEA with four monomers.

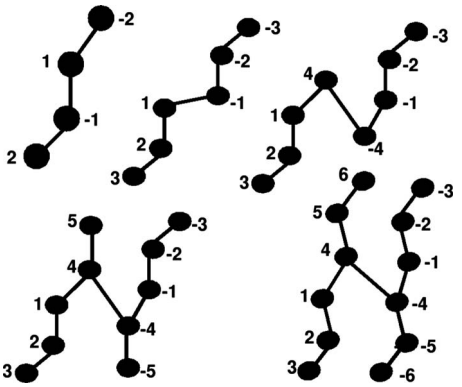

FIG. 2. Schematic diagram for building the PDEA system in our DMRG scheme is achieved by adding two sites at a time. Here, five DMRG steps leading to the building of two units of the PDEA are shown. Starting system size is four sites and we have shown the growth up to 12 sites. The new sites correspond to the highest absolute value of the site index.

As is well established now, electron correlations are long ranged in conjugated polymers.[16,17] The Hubbard model does not give the correct picture of the correlation effect in these systems. Hence, in this work, we incorporate the long-range Coulomb interactions within the PPP model[18] and study the effect of delocalized side chains on the optical gaps, two-photon absorption (TPA) gaps, and singlet-triplet (ST) gaps. We also carry out a comparative study of nonlinear optical (NLO) properties of the t-PA and PDEA employing the DMRG method.

II. MODEL HAMILTONIAN AND COMPUTATIONAL DETAILS

The PPP Hamiltonian and the associated parameters for modeling our system are given below:

$$\hat{H}_1 = \sum_{i,\sigma} \epsilon_i \hat{a}^{\dagger}_{i,\sigma} \hat{a}_{i,\sigma} + \sum_{\langle i,j\rangle,\sigma} t_{ij} (\hat{a}^{\dagger}_{i,\sigma} \hat{a}_{j,\sigma} + \text{H.c.}),$$

$$\hat{H}_2 = \sum_i U_i \hat{n}_{i,\uparrow} \hat{n}_{i,\downarrow},$$

$$\hat{H}_3 = \sum_{i>j} V_{i,j} (\hat{n}_i - 1)(\hat{n}_j - 1),$$

$$\hat{H}_{PPP} = \hat{H}_1 + \hat{H}_2 + \hat{H}_3. \quad (1)$$

Here $\hat{H}_1$ corresponds to the noninteracting part of the PPP model with ϵ_i being the site energy at site i set to zero in sp^2 carbon systems and t_{ij} being the transfer integral between bonded neighbors. The transfer integrals t_{ij} take the values $t_{ij}=t(1-\delta)$ for long bonds and $t_{ij}=t(1+\delta)$ for short bonds, with t set to -2.4 eV corresponding to the uniform C-C bond in benzene. Dimerization in the backbone and lateral chains is assumed to be the same to restrict the number parameters in the model Hamiltonian. An oligomer of PDEA with four units is shown Fig. 1. $\hat{H}_2$ corresponds to the Hubbard term with $U_C=11.26$ eV and $\hat{H}_3$ is the long-range Coulomb interaction part with $V_{i,j}$ obtained using Ohno parametrization.[10,19] It is well known that solving a quantum many-body Hamiltonian becomes a Herculean task because of the large Hilbert spaces spanned by correlated electron systems. Generally one- and quasi-one-dimensional conjugated polymers have large correlation lengths and to predict the physical properties in the thermodynamic limit, we should study systems of sizes larger than their correlation length. Thus, studying electronic states of polymers calls for methods that can handle large degrees of freedom. The DMRG method is one of the best techniques known for handling large one- and quasi-one-dimensional systems.[20,21] The DMRG method is based on discarding the insignificant degrees of freedom at each step. The degrees of freedom in the DMRG method correspond to the density-matrix eigenvectors (DMEVs) of the system block and their weights are given by their respective eigenvalues. The density matrix of a system (usually a half block) is constructed from the eigenvectors of the full system (superblock given by system block plus environment block) Hamiltonian by integrating out the degrees of freedom of the environment block. Accuracy of the result depends on the number, m, of DMEVs corresponding to the m highest eigenvalues that are retained for renormalization of the block Hamiltonian and required operators as well as on the route to the final structure, starting from a small superblock. We have grown the system along the lines of Yan and Mazumdar[15] shown in Fig. 2. In all our calculations, the final system size of PDEA corresponds to 12 units cells, except for the NLO study, where our calculations are limited to eight unit cells of PDEA. An infinite DMRG algorithm gives poor accuracy even with $m=200$ for the PDEA system and it is necessary to employ a finite DMRG algorithm until eigenvalues converge at every system size corresponding to integer unit cells of the PDEA polymer. We have checked the accuracy of the finite DMRG method for different values of m by studying the noninteracting model which can be solved numerically exactly. We find that $m=150$ gives accurate energies and beyond $m=150$, there is not much im-

provement in the accuracy. Therefore, all the studies we report in this work have been carried out using a finite DMRG scheme with a cutoff $m=150$. We have incorporated parity symmetry which exists in the total $M_s=0$, C_2 symmetry and electron-hole symmetry in our DMRG study to access specific states of interest.[22]

III. RESULTS AND DISCUSSION

This section is divided into two parts. In the first part, we review some existing results for various gaps and correlation functions. We compare these with our DMRG results obtained for the PPP model with long-range Coulomb interactions. We focus mainly on four states, the gs, the lowest dipole allowed (from gs) excited state, the lowest two-photon state, and the lowest triplet state. We compare our results for the PDEA chain with those of t-PA. We also study the effect of dimerization on the above properties in this part. In the second part, we carry out a comparative study of the dynamical optical polarizability and third harmonic generation (THG) coefficients of t-PA and PDEA. The effect of dimerization on linear polarizability and THG coefficients of the two systems is also compared.

Before analyzing our results we wish to point out that in all our studies, we assume that the PDEA and PA molecules are planar. In this case, the C_2 symmetry is identical to inversion symmetry of the molecules. All the states can therefore be labeled as A_g or B_u. The one-photon state is the lowest energy B_u state and the two-photon gap is from the ground state to the second lowest A_g state. It is also useful to give a brief overview of $2\ ^1A_g$-$1\ ^1B_u$ energy level crossing phenomenon in the linear chain which is now well understood. Consider a strongly correlated dimerized chain whose Hamiltonian is characterized by U/t and δ in the Hubbard limit. The model with only on-site interaction has an antiferromagnetic ground state in the large interaction limit. For $\delta=0$, in this limit, the $2\ ^1A_g$ state is degenerate with the gs and so is the lowest triplet state. The optical gap to $1\ ^1B_u$ state is infinite in this limit as the $1\ ^1B_u$ state does not contain any configuration with exactly one electron at each site. For $\delta\neq 0$ the $2\ ^1A_g$ state is no longer degenerate with the gs and a gap also opens up between the gs and the lowest triplet state. The gap to $2\ ^1A_g$ state is nearly twice the gap to the triplet state and it has been shown by many workers that $2\ ^1A_g$ state can be described as consisting of two triplet excitons.[23] If the range of Coulomb interactions are extended to the nearest neighbor, with strength V then for $\delta=0$ and finite U/t, in the limit $V<U/2$, the gs does not have a spin gap and the spin gap opens as $4t^2(1-\delta)/(U-V)$ for small δ.[24] For $V/t>U/2t$, the ground state is a charge-density wave state with vanishing optical gap, a finite spin gap, and a two-photon gap. For intermediate values of correlations, the $2\ ^1A_g$ gap increases more rapidly with δ than the optical gap since the $2\ ^1A_g$ state can be described as two electron–two hole excitation. With increasing correlation strength the $1\ ^1B_u$ gap increases rapidly, while the $2\ ^1A_g$ gap decreases. Besides, the excited states have different extent of relaxation depending upon properties such as bond order and charge-density distributions. This also leads to sharper decreases in the $1\ ^1B_u$ energy with increasing chain length while the $2\ ^1A_g$ gap saturates rapidly with system size.

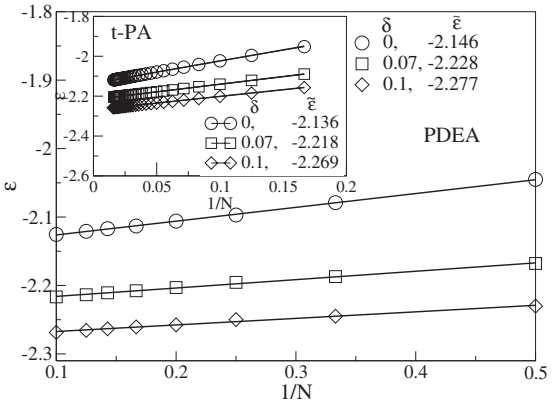

FIG. 3. Energy per unit cell, ϵ, of PDEA vs $1/N$, where N is number of PDEA units for different values of bond alteration, δ. Shown in the inset are the results for t-PA. $\tilde{\epsilon}$ denotes extrapolated energy per unit cell to the infinite limit.

We now turn our attention to the PDEA chains. In the polymer limit, the dimerization of the chain can be described by a single value of δ, since all the backbone double bonds are equivalent in the polymer limit and so are all the backbone single bonds. However, the side chains are finite in extent and the δ parameter for the side chains should be different. However, for the sake of dealing with fewer parameters, we have assumed that the δ for the side chains is the same as the δ for the backbone. In correlated models, it is well known that the contribution of the one-particle gap to the actual excitation gap in the spectrum is small and small differences in δ will not affect the gaps in any significant way.

A. Low-lying states

We have plotted the gs energy per unit cell for PDEA in Fig. 3 for different δ values and shown in the inset are the same for t-PA. We note that the PDEA gs energy per unit cell saturates rapidly with increasing oligomer length. This implies that studies up to about ten unit cells of PDEA are enough to obtain reliable properties of the infinite system.

In Fig. 4, we present the optical gap Δ_{op} vs $1/N$ plot for oligomers of PDEA and compare it with the optical gap in t-PA for different dimerizations, δ. We note that the optical gap of PDEA saturates very rapidly for all values of δ, unlike in the case of t-PA, where saturation length depends upon δ and even for $\delta=0.1$ saturation occurs only slowly. We also note that in the case of PDEA, the optical gap changes more gradually with increase in dimerization when compared to t-PA. For a uniform system the t-PA optical gap Δ_{op}^{∞} is slightly smaller than in PDEA. However, even at $\delta=0.07$, the t-PA Δ_{op}^{∞} is larger than that in PDEA. Although the optical gap in PDEA for 7% bond alternation (corresponding to experimentally found bond alternation in t-PA) is slightly lower than that in t-PA, these results are contrary to the initial expectation of very low optical gap in PDEA.[15] This implies that $1B_u$ excitonic states in PDEA are similar to those in t-PA.

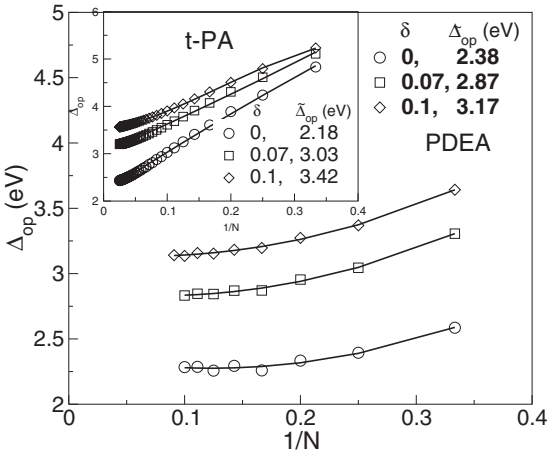

FIG. 4. Optical gap Δ_{op} vs $1/N$ (N is number of PDEA units) for different values of bond alteration, δ. Inset: Δ_{op} of t-PA vs $1/N$. $\tilde{\Delta}_{op}$ is the optical gap extrapolated to the infinite polymer limit.

In Fig. 5, we present the TPA gaps, Δ_{TPA}, of PDEA for different dimerizations and again for comparison, we have also shown the TPA gap in t-PA. In this case, unlike with Δ_{op}, there is no saturation of the gap for $\delta=0$. Another interesting feature is that the TPA gap in PDEA extrapolates to a finite value in the thermodynamic limit for $\delta=0$ ($\Delta^{\infty}_{TPA}=0.97$) while for t-PA this gap almost vanishes for uniform chains. It is well known that for $\delta=0$ and $U=0$, the TPA gap of t-PA should be zero. For finite U, again the $2A_g$ is in the covalent subspace; it vanishes in t-PA. However, in PDEA we do not expect for $\delta=0$, $U=0$ TPA gap to vanish as the PDEA unit cell has more atoms and the molecular orbitals in the unit cell will have large energy separation even for $\delta=0$. In the extended systems, we expect the resulting bands to have a nonzero band gap and a semiconducting behavior. Again as with Δ^{∞}_{op}, Δ^{∞}_{TPA} of the t-PA chain increases more rapidly with increase in δ and these gaps are larger in t-PA than in PDEA. However, in all the cases the TPA gap is smaller than the corresponding optical gap showing that the PDEA system is not strongly fluorescent like the t-PA system.

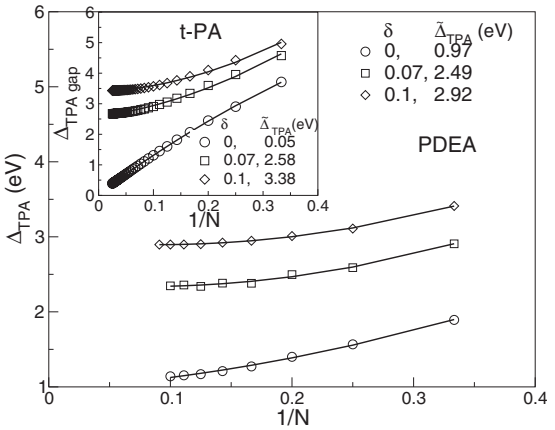

FIG. 5. TPA gap to the $2A_g$ state, (Δ_{TPA}), vs $1/N$ (N is number of PDEA units) for three values of alteration δ. Inset shows Δ_{TPA} vs $1/N$ for t-PA. $\tilde{\Delta}_{TPA}$ denotes extrapolated TPA gap to the polymer limit.

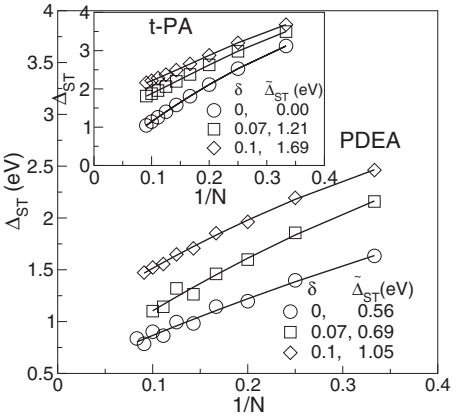

FIG. 6. Singlet-triplet gap Δ_{ST} vs $1/N$, where N is number of PDEA units for different values of δ; Δ_{ST} of t-PA plot is shown in the inset. $\tilde{\Delta}_{ST}$ denotes extrapolated singlet-triplet gap (Δ^{∞}_{ST}).

In Fig. 6, we have shown the ST gap, Δ_{ST}, of the PDEA and t-PA systems as a function of inverse system size. As is expected from earlier calculations as well as on physical basis, the Δ^{∞}_{ST} of t-PA for uniform chain extrapolates to zero. However, Δ_{ST}, Δ^{∞}_{ST} of PDEA for $\delta=0$ is 0.56 eV. The ST gap increases with δ for both t-PA and PDEA. The increase is again more rapid in the case of t-PA compared to PDEA. In the case of t-PA, $2\Delta^{\infty}_{ST}\approx\Delta^{\infty}_{TPA}$ is in agreement with the description of the $2\,{}^1A_g$ state as composed of two triplet excitons for all δ values we have studied. However, in the case of PDEA, the energy gap to $2\,{}^1A_g$ state and the ST gap for nonzero value of δ depends upon system size. The extrapolated gaps of t-PA and PDEA are summarized in Table I for convenience. We present in Table II transition dipoles of t-PA and PDEA for two different oligomer sizes.

We note that both in t-PA and in PDEA, the absorptions are both x and y polarized. Our x axis passes through the midpoints of the backbone C-C bonds and the y axis is perpendicular to the x axis in the plane of the paper. This is because both t-PDEA and t-PA belong to the C_2 point group and in this group the optically allowed B state transforms as x and y and the ground state transforms as z. t-PA has a stronger absorption cross section than PDEA at both system sizes for all dimerizations. With increase in dimerization the absorption cross section reduces slightly compared to their undimerized values. The absorption intensities in both t-PA and PDEA scale approximately linearly with system size.

To understand the nature of excited states, we have computed charge-charge correlation functions (CCCFs), spin-

TABLE I. Extrapolated values of Δ^{∞}_{TPA}, Δ^{∞}_{op}, and Δ^{∞}_{ST} of PDEA and t-PA are compared for different values of δ.

	PDEA			t-PA		
δ	Δ^{∞}_{op} (eV)	Δ^{∞}_{TPA} (eV)	Δ^{∞}_{ST} (eV)	Δ^{∞}_{op} (eV)	Δ^{∞}_{TPA} (eV)	Δ^{∞}_{ST} (eV)
0.00	2.38	0.97	0.56	2.18	0.05	0.00
0.07	2.87	2.49	0.69	3.03	2.58	1.21
0.10	3.17	2.92	1.05	3.42	3.38	1.69

TABLE II. Comparison of transition dipole moments ($|\mu_x|$ and $|\mu_y|$) of t-PA and PDEA for different values of δ. Transition dipole moments are given for two system sizes, N, in both cases.

		PDEA			t-PA		
N	δ	Δ_{op}^{∞} (eV)	$\lvert\mu_x\rvert$ (a.u.)	$\lvert\mu_y\rvert$ (a.u.)	Δ_{op}^{∞} (eV)	$\lvert\mu_x\rvert$ (a.u.)	$\lvert\mu_y\rvert$ (a.u.)
4	0.00	2.394	0.692	0.227	4.237	1.829	0.394
4	0.07	3.468	0.781	0.682	4.615	1.724	0.417
4	0.10	3.369	0.940	0.614	4.797	1.671	0.420
11	0.00	2.284	1.281	0.195	2.939	3.571	0.386
11	0.07	2.832	1.585	0.629	3.530	3.162	0.529
11	0.10	3.141	1.846	0.886	3.851	2.990	0.554

spin correlation functions, and bond orders in all the states. Besides these, we have also computed spin densities in the triplet state. The correlations are calculated with reference to the latest site added on one half of the full system with all the sites on the other half. The site numbering adopted for the intersite-correlation calculations is shown in Fig. 7 and that for bond orders in Fig. 8.

In Fig. 9, we have shown the variation in the CCCF between the reference site and backbone sites on the right-half system for 12 PDEA units (consisting of 72 sites). The CCCF is shown for the three states of interest, namely, the gs, the dipole connected lowest singlet state ($1B_u$), and lowest two-photon state ($2A_g$) for two different values of δ (Fig. 10). We also compare it with the t-PA dependence on distance. We find that the charge correlations are extremely short ranged in both systems. For δ=0, in PDEA the dependence is almost identical for the gs and the $2A_g$ state. However, for the dimerized PDEA case (nonzero δ), the TPA state shows slightly larger variation than the gs. The $1B_u$ CCCF

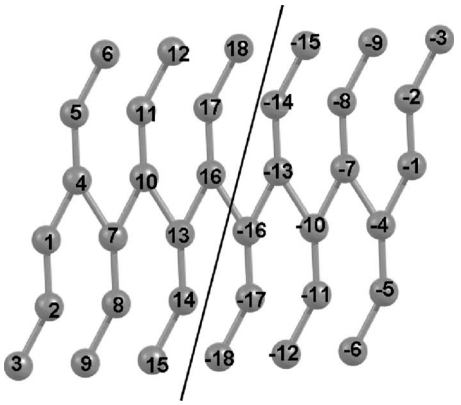

FIG. 7. Numbering scheme adopted in the presentation of correlation functions. In a 12N system with $N/2$ unit cells on the left and $N/2$ unit cells on the right, the latest site added on the left half of the full system is numbered 6N. Correlations between properties on this site and sites "j" on the right half, namely, $j=-1,-2,\ldots,-6N$ are reported. For the right half-block, the transverse sites correspond to site numbers $-6p$, $-(6p-1)$, $-(6p-4)$, and $-(6p-5)$. Sites $-(6p-2)$ and $-(6p-3)$ are the backbone sites. We consider $p=1,2,\ldots,6$.

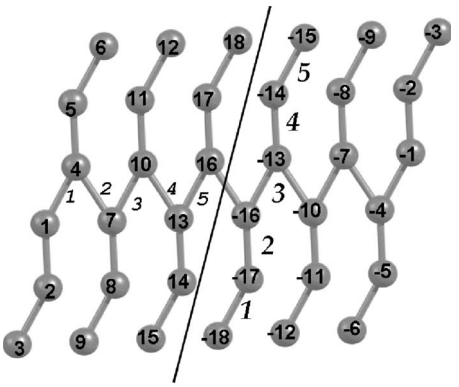

FIG. 8. Numbering scheme for bond orders. The bond orders for the backbone are numbered sequentially from 1 to $(N-1)$ starting from the end of the backbone. Similarly bond orders for the side chains are numbered sequentially from top to bottom. The backbone numbering and side chain numbering are shown in different fonts on the left and right half-blocks, respectively.

variation is also enhanced with dimerization. The correlations in t-PA fall off more slowly than in PDEA in all the states. The behavior of the CCCF in different states of PDEA is in keeping with the fact that $1B_u$ state is an ionic state while gs and TPA states are more covalent. The side chain correlations are also quite short ranged.

We now turn our attention to the spin densities and spin-spin correlations in the triplet state. We note that we have large positive spin density on the odd numbered sites on the backbone and the largest negative spin densities are also found on the even numbered backbone sites in the lowest triplet state. On the side chain the spin densities alternate such that from one end to the other the spin densities alternate in sign. For the triplet state with δ=0.1 the magnitudes of the spin densities are smaller and the density is smeared over the entire system.

In Fig. 11, we have shown the spin-spin correlation of the PDEA system in the lowest triplet state. Again, as with the

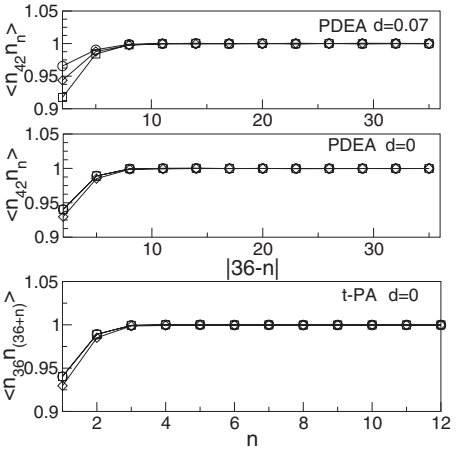

FIG. 9. Charge-charge correlation function from the reference site 36 of the 72 site system to sites along the backbone (see Fig. 7) of the left-half block. For δ=0, charge-charge correlation function of t-PA [in panel (a)] and PDEA [in panel (b)] for the gs (○–○), the $2A_g$ state (□–□), and the $1B_u$ state (◇–◇) are shown. In panel (c), for these quantities are shown for PDEA for δ=0.07.

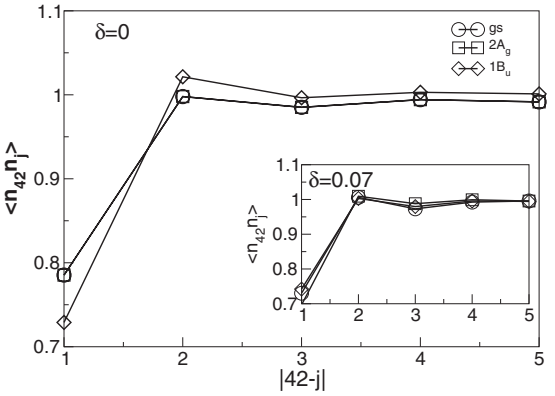

FIG. 10. Charge-charge correlation function of PDEA in gs, $2A_g$, and $1B_u$ states with respect to the referenced site within a single unit cell in the middle for two different δ values. ○–○ denotes gs, □–□ denotes $2A_g$, and ◇–◇ $1B_u$.

CCCFs, in PDEA, the spin correlation function is also short ranged compared to that of the triplet state in t-PA. The triplet excitation in PDEA seems to be delocalized onto the nearest neighbors both along the backbone and along the side chain, and beyond the nearest neighbor correlations fall off sharply. The spin correlation amplitude in PDEA is smaller than in t-PA. All these results point toward shorter π coherence in PDEA than in t-PA, for similar dimerization strengths.

In Fig. 12, we show the variation in bond orders for different bonds in the states of interest for PDEA with and without dimerization and compare these results with t-PA at δ=0.07. We note that bond alternation in t-PA has a large amplitude for all the states. In the gs and $1B_u$ states of t-PA, the terminal bonds are stronger while in the triplet and $2A_g$ states the terminal bonds are weaker. The similarity between $2A_g$ and triplet states can also be understood from the fact that $2A_g$ state consists of two triplets. The two free radicals in the triplet prefer to be at the ends resulting in reduction in the

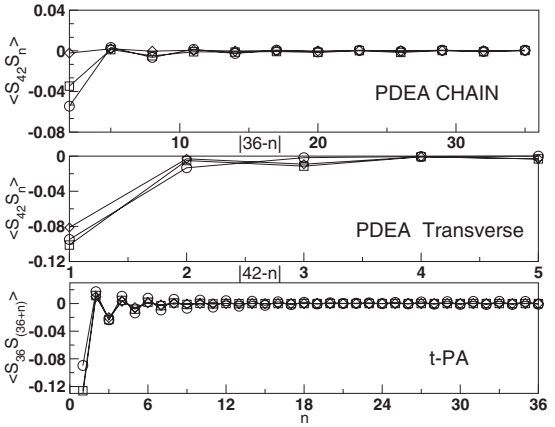

FIG. 11. Spin-spin correlation in lowest triplet state for three different values δ=0, 0.07, and 0.1 for a PDEA and PA systems of 72 sites. Top panel is for backbone correlation, middle panel is for transverse sites, and bottom is for t-PA. Site numberings are the same as in Fig. 7. ○–○ corresponds to δ=0, □–□ to δ=0.07, and ◇–◇ to δ=0.1.

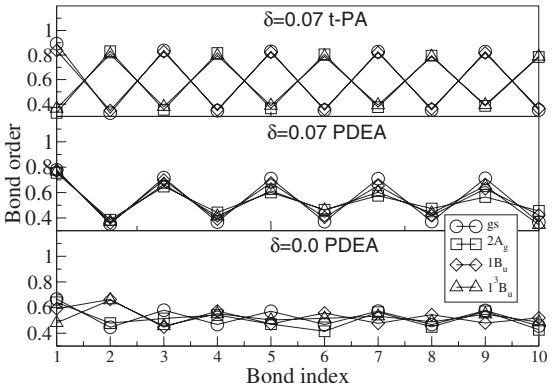

FIG. 12. Bond orders along the backbone of PDEA and t-PA. ○–○ is for the ground state, □–□ for the $2A_g$ state, ◇–◇ for the $1B_u$ state, and △–△ for the lowest triplet state. Bond numberings are as shown in Fig. 8.

effective bond order. However, in PDEA, all the four states have similar bond orders at δ=0.07 while for δ=0, the behavior is comparable to t-PA albeit with smaller amplitude in the oscillation. In the alternating PDEA, the amplitude of oscillation is stronger and dies down slowly as we approach the center of the system. Besides, bond order oscillations in the gs die down more slowly as we move toward the interior of the system compared to that in $2A_g$ state.

In Fig. 13, we show the bond orders along the side chain in one of the central units of the 72 site system. The ethylinic bonds at the ends are the strongest while the bond between the backbone and the ethylene unit is the weakest. The differences in the bond orders of different states are mainly in the backbone. The CCCFs and bond orders in different states show that these states differ mainly along the backbone.

B. Dynamical optical properties

We have also computed the frequency-dependent polarizability $\alpha_{ij}(\omega)$ and THG coefficients $\gamma_{ijkl}(\omega,\omega,\omega)$ of PDEA and compared the same with t-PA. We have chosen to com-

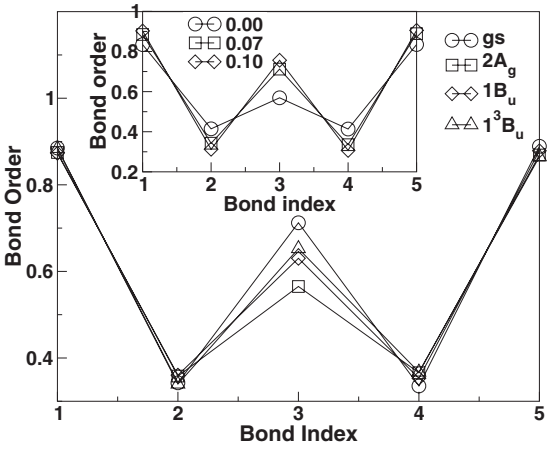

FIG. 13. Bond orders along the backbone and along the transverse direction in the PDEA in gs, $2A_g$, $1B_u$, and triplet states ($1\,^3B_u$) for δ=0. Inset: gs bond orders for different δ values. Bond numberings are as shown in Fig. 8.

pute THG coefficients since they are most widely studied in the context of conjugated polymers and the materials showing large THG response are important for deep UV conversion. We have employed the correction vector (CV) approach[10] within the DMRG scheme[25,26] for computing these optical response coefficients. The DMRG technique as originally conceived uses an optimal space for constructing the renormalized Hamiltonian matrix for a specific state while the CV method incorporates all the excitations of the model without explicit computation of the excited states. In order to have both gs and excited states represented in the DMRG space, we employ DMEV from an average reduced density matrix. The averaged reduced density matrix is constructed as the simple average of reduced density matrix of gs and that from the correction vector. The CV-DMRG method has now proved to be the method of choice for computing frequency-dependent response functions. This method is employed for the computation of the polarizability $\alpha_{ij}(\omega)$ and THG coefficients $\gamma_{ijkl}(\omega,\omega,\omega)$.[26] In the case of PDEA, these calculations have been carried out on a system with eight unit cells. The t-PA system studied contains 24 unit cells. Both the systems have the same number of sp^2 C atoms in conjugation and thus permit comparison of the response coefficients. Since it is difficult to compare coefficients, component by component, we have compared tumbling averaged response coefficients defined as

$$\alpha_{av}(\omega) = \sum_{i=1}^{3} \frac{1}{3}\alpha_{ii}(\omega),$$

$$\gamma_{av}(\omega,\omega,\omega) = \sum_{i,j=1}^{3} \frac{1}{15}[2\gamma_{iijj}(\omega,\omega,\omega) + \gamma_{ijji}(\omega,\omega,\omega)]. \quad (2)$$

We have computed the response coefficients for three different frequencies and three different dimerizations. The response coefficients assume large values close to resonances and calculations at frequencies away from resonance are necessary to infer relative nonresonant response coefficients for comparison between the two systems. Computing the linear and nonlinear optic coefficients at different frequencies in PDEA can give information about the backbone and side chain excitations. However, since our aim in this study is to compare PDEA and PA we have chosen to compute these quantities at a few common frequencies for both the systems. We have computed the optic response coefficients at two low excitation frequencies to confirm that we are away from resonance. The third frequency corresponds to the Nd:YAG laser frequency.

In Table III, we present the results for tumbling averaged $\alpha_{av}(\omega)$ and $\gamma_{av}(\omega,\omega,\omega)$ for different dimerizations and excitation frequencies. We have chosen to compare the properties across systems with different optical gaps simply because we are interested in comparing the PDEA and t-PA systems. Besides, it is well known that just the lowest-lying dipole allowed excitation does not control the linear or nonlinear optic responses of a material. We note that $\alpha_{av}(\omega)$ values for PDEA are always smaller than those of t-PA by nearly an order of magnitude in all cases. In both PDEA and t-PA $\alpha_{av}(\omega)$ is computed below the first resonance frequency. Thus, we do not see any significant dependence of $\alpha_{av}(\omega)$ on the excitation frequency ω. We note that increasing δ reduces $\alpha_{av}(\omega)$ in all cases shown in Table III. This can be explained by the fact that the optical gap increases with δ and thus the system becomes less polarizable. The $\gamma_{av}(\omega,\omega,\omega)$ values also show a similar trend. The tumbling averaged THG coefficient in PDEA is smaller by a factor between 10^2–10^4 than that of t-PA. The $\gamma_{av}(\omega,\omega,\omega)$ values have stronger frequency dependence since they contain terms which can become singular due to two-photon or three-photon resonances. But, from Table III we can still infer that the nonresonant γ_{av} of PDEA is about two orders of magnitude smaller than the t-PA γ_{av} value. While both t-PA and PDEA systems studied by us have the same number of carbon atoms in conjugation, in t-PA the conjugation is completely one dimensional, while in PDEA the conjugation length is eight carbons long along the backbone and six carbons long along the side chain. The scaling of $\gamma_{av}(\omega,\omega,\omega)$ with conjugation length has an exponent of 3.5 (Ref. 10) and thus contributes overwhelmingly to the larger $\gamma_{av}(\omega,\omega,\omega)$ observed in t-PA. We infer that PDEA cannot substitute t-PA in applications that require a strong nonlinear optic response property.

TABLE III. Comparison of NLO properties of PDEA and t-PA for different excitation frequencies and dimerizations. In both systems, we have 48 carbon atoms in conjugation.

		PDEA		t-PA	
$\hbar\omega$ (eV)	δ	$\alpha_{av}(\omega)$ (a.u.)	$\gamma_{av}(\omega,\omega,\omega)$ 10^4 (a.u.)	$\alpha_{av}(\omega)$ (a.u.)	$\gamma_{av}(\omega,\omega,\omega)$ 10^4 (a.u.)
0.500	0.000	43.56	2.680	531.1	2109
0.800	0.000	39.64	5.363	547.2	6350
1.170	0.000	41.95	0.9469	608.9	5960
0.500	0.070	37.43	1.344	323.0	289.2
0.800	0.070	37.82	1.716	334.0	644.1
1.170	0.070	38.59	2.615	357.0	9417
0.500	0.100	28.80	1.038	274.0	92.77
0.800	0.100	29.05	1.226	281.2	192.9
1.170	0.100	29.53	1.038	287.1	1943

IV. SUMMARY

We have employed the DMRG technique to study the important electronic states of PDEA and have compared the properties of these states with the corresponding states of t-PA. We note that the excitation gaps in PDEA saturate rapidly with system size. The $2A_g$ (TPA) gap in PDEA is nonzero even for $\delta=0$ unlike with t-PA. However, for nonzero δ values the $1B_u$ state, $2A_g$ state, as well as the lowest triplet state all have larger gaps in t-PA than for the corresponding states in PDEA. The $2A_g$ state in PDEA also lies below the $1B_u$ state and hence PDEA systems will also be only weakly fluorescent. The $2A_g$ gap as well as the ST gap in PDEA do not vanish for $\delta=0$ unlike in t-PA.[27] This is attributed to a different single-particle spectrum in PDEA compared to

t-PA. The $2A_g$ state in PDEA cannot be described as a composite of two triplet states unlike with t-PA. The charge and spin correlations in PDEA have very short correlation lengths consistent with the rapid saturation of the excitation gaps to the low-lying states with system size. The bond order studies of PDEA also show that the relaxations in the geometry of the excited states are small and are therefore expected to have small Stokes shifts. The linear and nonlinear optic response coefficients of PDEA are smaller by a factor of 10 and 10^2-10^4, respectively, compared to t-PA values. This can be attributed to shorter π-conjugation length in PDEA compared to t-PA for oligomers of similar molecular weights.

ACKNOWLEDGMENTS

M.K. thanks UGC India for financial support. S.R. thanks DST for the J. C. Bose National grant. This work was supported in part by a grant from DST, India (Grant No. SR/S2/CMP-24/2003).

[1] J. L. Bredas and R. Silbey, *Conjugated Polymers: The Novel Science and Technology of Highly Conducting and Nonlinear Optically Active Materials* (Kluwer Academic, Dordrecht, 1991).
[2] J. W. Blatchford and A. J. Epstein, Am. J. Phys. **64**, 120 (1996).
[3] D. de Leeuw, Phys. World **12**, 31 (1999).
[4] J. Kido, Phys. World **12**, 27 (1999).
[5] M. Kasha, Radiat. Res. **20**, 55 (1963).
[6] Z. G. Soos, S. Ramasesha, and D. S. Galváo, Phys. Rev. Lett. **71**, 1609 (1993).
[7] Y. M. Huang and W. Ge, Appl. Phys. Lett. **75**, 4094 (1999).
[8] J. H. Burroughes, D. D. C. Bradley, A. R. Brown, R. N. Marks, K. Mackay, R. H. Friend, P. L. Burn, and A. B. Holmes, Nature (London) **347**, 539 (1990).
[9] B. S. Hudson and B. E. Kohler, Chem. Phys. Lett. **14**, 299 (1972).
[10] Z. G. Soos and S. Ramasesha, J. Chem. Phys. **90**, 1067 (1989).
[11] K. Schulten, I. Ohmine, and M. Karplus, J. Chem. Phys. **64**, 4422 (1976).
[12] Z. Shuai, J. L. Brédas, S. K. Pati, and S. Ramasesha, Phys. Rev. B **56**, 9298 (1997).
[13] A. Shukla and S. Mazumdar, Phys. Rev. Lett. **83**, 3944 (1999).
[14] S. Dallakyan, M. Chandross, and S. Mazumdar, Phys. Rev. B **68**, 075204 (2003).
[15] Y. Yan and S. Mazumdar, Phys. Rev. B **72**, 212201 (2005).
[16] C. Raghu, Y. Anusooya Pati, and S. Ramasesha, Phys. Rev. B **66**, 035116 (2002).
[17] M. Kumar, S. Ramasesha, R. A. Pascal, Jr., and Z. G. Soos, Europhys. Lett. **83**, 37001 (2008).
[18] R. Pariser and R. G. Parr, J. Chem. Phys. **21**, 466 (1953); **21**, 767 (1953).
[19] K. Ohno, Theor. Chim. Acta **2**, 219 (1964).
[20] S. R. White, Phys. Rev. Lett. **69**, 2863 (1992).
[21] S. R. White, Phys. Rev. B **48**, 10345 (1993).
[22] S. Ramasesha, S. K. Pati, Z. Shuai, and J. L. Brédas, Adv. Quantum Chem. **38**, 121 (2000).
[23] P. Tavan and K. Schulten, Phys. Rev. B **36**, 4337 (1987).
[24] M. Kumar, S. Ramasesha, and Z. G. Soos, Phys. Rev. B **79**, 035102 (2009).
[25] S. Ramasesha, S. K. Pati, H. R. Krishnamurthy, Z. Shuai, and J.-L. Brédas, Synth. Met. **85**, 1019 (1997).
[26] S. K. Pati, S. Ramasesha, Z. Shuai, and J. L. Brédas, Phys. Rev. B **59**, 14827 (1999).
[27] M. Kumar, S. Ramasesha, Diptiman Sen, and Z. G. Soos, Phys. Rev. B **75**, 052404 (2007).